



**STUDY OF  $\text{Bi}_{0.5}\text{NA}_{0.5}\text{TiO}_3$  SYSTEM DOPED WITH  $\text{La}^{3+}$  OBTAINED BY ACETIC ACID ROUTE IN SOL-GEL PROCESS**

**ESTUDIO DEL SISTEMA  $\text{Bi}_{0.5}\text{NA}_{0.5}\text{TiO}_3$  DOPADO CON  $\text{La}^{3+}$  OBTENIDO MEDIANTE LA RUTA DE ÁCIDO ACÉTICO EN PROCESO SOL-GEL**

K. M. Moya-Canul<sup>1,2</sup> and J.M. Yáñez-Limón<sup>1\*</sup>

<sup>1</sup>Universidad de Investigación de Tecnología Experimental Yachay, Ciudad del conocimiento, Hacienda San José s/n, Cantón San Miguel de Urcuquí, Imbabura, Ecuador.

<sup>2</sup>Centro de Investigación y de Estudios Avanzados del I.P.N.-Unidad Querétaro, Libramiento Norponiente No. 2000, Fracc. Real de Juriquilla, 76230 Querétaro, Querétaro, México.

Received: April 12, 2019; Accepted: June 22, 2019

**Abstract**

This work studies the system  $\text{Bi}_{0.5}\text{NA}_{0.5}\text{TiO}_3$  (BNT) doped with lanthanum ( $\text{La}^{3+}$ ) at molar concentrations 0.0, 0.3, 0.6, 0.8, 1.0, 3.0 and 6.0. The samples were synthesized by the Sol-gel method using the acetic acid route. The bulk samples were calcined at 700 °C/1hr in order to obtain the perovskite phase, and finally the samples were sintered at 1050 °C/1hr, obtaining density values between 90 and 92% with respect to the theoretical density. The La doping effect in the BNT system was analyzed using X-ray diffraction (DRX), Scanning electron microscopy (SEM), Ferroelectric hysteresis curves and Raman spectroscopy. The samples show a crystalline rhombohedral structure and is observed a decreasing behavior of the grain size for La concentrations greater than 0.3%. After the incorporation of 0.6% lanthanum concentration, the presence of the pyrochlore phase of  $\text{Bi}_2\text{Ti}_2\text{O}_7$  is observed. The best ferroelectric properties were obtained for BNT doped with lanthanum ( $\text{La}^{3+}$ ) at 6% in which a rhombohedral structure and traces of pyrochlore phases were obtained. This sample presented maximum polarization ( $P_m$ ) of 22.55  $\mu\text{C}/\text{cm}^2$ , remnant polarization ( $P_r$ ) of 22.06  $\mu\text{C}/\text{cm}^2$  and a coercive field ( $E_c$ ) of 25 kV/cm.

**Keywords:** BNT, ferroelectric ceramics, piezoelectrics, multifunctional materials

**Resumen**

Este trabajo estudia el sistema  $\text{Bi}_{0.5}\text{NA}_{0.5}\text{TiO}_3$  (BNT) dopado con lantano ( $\text{La}^{3+}$ ) a concentraciones molares de 0.0, 0.3, 0.6, 0.8, 1.0, 3.0 and 6.0. Las muestras fueron sintetizadas mediante sol-gel usando la ruta del ácido acético. Las muestras en volumen fueron calcinadas a 700 °C/1hr con la finalidad de obtener la fase perovskita, y finalmente fueron sinterizadas a 1050 °C/1hr, obteniendo valores de densidad entre 90 y 92% con respecto a la densidad teórica. El efecto del dopaje con lantano en el sistema BNT fue analizado utilizando difracción de rayos x (DRX), microscopía electrónica de barrido (MEB), curvas de histeresis ferroeléctrica y espectroscopía Raman. Se obtuvieron muestras con estructura cristalina romboédrica y se presentó una disminución en el tamaño de grano con respecto a las concentraciones de lantano mayores a 0.3%. A partir de las concentraciones de lantano al 0.6% es posible observar la aparición de la fase pirocloro  $\text{Bi}_2\text{Ti}_2\text{O}_7$ . Las mejores propiedades ferroeléctricas fueron obtenidas para el BNT dopado con lantano ( $\text{La}^{3+}$ ) al 6%, en el cual la fase perovskita romboédrica y trazas de la fase pirocloro coexisten. Esta muestra presentó una polarización máxima de ( $P_m$ ) 22.55  $\mu\text{C}/\text{cm}^2$ , Polarización remanente de ( $P_r$ ) 22.06  $\mu\text{C}/\text{cm}^2$  y un campo coercitivo de ( $E_c$ ) de 25 kV/cm.

**Palabras clave:** BNT, cerámicos ferroeléctricos, piezoelectrics, materiales multifuncionales.

**1 Introduction**

Ferroelectric materials are essential components for a broad spectrum of devices. This is due to its excellent multifunctional properties such as pyroelectric, piezoelectric, ferroelectric, dielectric and electro-optical properties (Haertling, 1999 and Fernández,

2010). After the presence of a morphotropic phase limit was identified in the ferroelectric system  $\text{PbZr}_x\text{Ti}_{1-x}\text{O}_3$  (PZT), its study became popular, due to the presence of the the maximum dielectric and piezoelectric properties in their respective morphotropic limits in various ferroelectric systems (Mayen *et al.*, 2013; Jaffe *et al.*, 1971 and Jaffe *et al.*, 1965).

\* Corresponding author. E-mail: jmyanez@cinvestav.mx

<https://doi.org/10.24275/rmiq/Mat591>

issn-e: 2395-8472

For this reason, the PZT, since its discovery, dominates the market until today. However, the presence of lead within its structure represents health risks, because it is highly toxic. Moreover, its toxicity is further increased due to its volatilization at high temperature processing, particularly during calcination and sintering, causing environmental contamination and damage to health (Yugong *et al.*, 2009, Rodel *et al.*, 2009 and Peng *et al.*, 2010). Due to these inherent defects, lead-based ceramics are not the most suitable in applications that require good electrical and mechanical resistance. Thus, even though the PZT is one of the materials with the best ferroelectric properties, it is necessary to develop lead-free ferroelectric ceramics that are friendly to the environment, to human health and that have good physical properties at the same time. On the other hand, Bismuth sodium titanate (BNT), discovered by Smolensky in 1960 (Smolensky *et al.*, 1961 and Jaita *et al.*, 2011) is a lead-free ferroelectric material of great importance in terms of its electrical and mechanical properties. It has a perovskite structure, which can be obtained from the reaction of precursor materials in solid state or via sol gel. It is common causing the formation of intermediate phases such as  $\text{Bi}_2\text{Ti}_2\text{O}_7$  coming from the bismuth and titanium oxides and from which, it has been found to have great influence on the electrical and dielectric properties of BNT (Espinoza *et al.*, 2017). BNT system has been subjected to different studies for technological applications in the last years, for example, due to its functionality as an energy collector in the BNT-BT system doped with Zirconium, was reported a significant improvement in its pyroelectric coefficient, contributing greatly to improving the energy harvesting performance when designing the phase structure and the phase transition temperature (Meng *et al.*, 2019).

Another recent study of the BNT-6BT system doped with Lanthanum, shows that it is possible to increase the dielectric constant near the ambient temperature, and change the transition temperature from ferroelectric to relaxor in a lower temperature as the lanthanum content increases ( $> 0.1$ ). This considerably decreases the temperature change of the electrocaloric effect, which indicates that it is a promising lead-free material for the application of solid-state cooling systems (Lucheng *et al.*, 2018).

The BNT system has been studied extensively due to its excellent piezoelectric properties, however pure BNT is difficult to polarize because it has large coercive fields and high conductivity, which is why

many systems have been created based on BNT as BNT-BT, BNT-BKT, and BNT-BKT-BT. (Xing Yu K. *et al.*, 2019 and Martínez J.R. *et al.* 1999) seeking to modify and improve such characteristics. In BNT has been reported remaining polarization values  $P_r$ , of  $38 \mu\text{C}/\text{cm}^2$ , Curie temperature of  $320 \text{ }^\circ\text{C}$  and a coercive field of  $73 \text{ kV}/\text{cm}$  (Mei ling *et al.*, 2014).

In this work we study the system  $\text{Bi}_{0.5}\text{Na}_{0.5}\text{TiO}_3$  (BNT) and BNT doped with lanthanum ( $\text{La}^{3+}$ ) (BNTL). In order to analyze the effect of La incorporation on the ferroelectric properties of BNT, given that, as it has been found that BNT doping with lanthanum by solid-state reaction benefits the densification of ceramics ( $\leq 95\%$  of the theoretical density) although it reduces the grain size (Khairunisak, 2016). Firstly, we will analyze the experimental part of the BNT synthesis using the sol-gel technique by the acetic acid route; followed by a pyrolysis, calcination and sintering process. This wet chemical technique, show great versatility because is easy to use, accessible and more economical with respect to the vacuum techniques (Tirado, 2015). Subsequently, the structural results obtained by XRD and Raman are analyzed, and finally, the effect of the concentration of doping of Lanthanum on the Ferroelectric properties of the obtained samples is studied.

## 2 Materials and methods

### 2.1 Preparation of the precursor solution

To prepare the solution of BNT and BNT doped with lanthanum (BNTL), alkoxides were used as precursors; sodium acetate ( $\text{C}_2\text{H}_3\text{NaO}_2$ ) 99%, bismuth acetate ( $\text{C}_6\text{H}_9\text{BiO}_6$ ), titanium isopropoxide ( $\text{C}_{12}\text{H}_{28}\text{O}_4\text{Ti}$ ), and lanthanum acetate ( $\text{C}_6\text{H}_9\text{LaO}_6$ ), all with 99.99% of purity. The solvents used were acetic acid ( $\text{C}_2\text{H}_4\text{O}_2$ ) 99.7%, 2-propanol ( $\text{C}_3\text{H}_8\text{O}$ ) 99.5%, and acetylacetone ( $\text{C}_5\text{H}_8\text{O}_2$ ) 99%, all obtained from Sigma Aldrich Inc.

To prepare the precursor solution, three solutions of 1M concentration are prepared. Solution 1 (sodium acetate and acetic acid) was heated at  $50 \text{ }^\circ\text{C}$  and remained under stirring until it dissolved. Solution 2 (bismuth acetate and acetic acid) was heated at  $80 \text{ }^\circ\text{C}$  with vigorous stirring until dissolved. Subsequently, solution 1 and 2 were mixed and their agitation was continued. Meanwhile, solution 3 (titanium isopropoxide, 2-propanol and acetylacetone

as the chelating agent) was stirred at room temperature and then added dropwise to solution 1-2 (previously mixed). In the case of the BNT solution doped with lanthanum, the respective concentrations of lanthanum are added to solution 1, and the same procedure is performed (Cernea *et al.*, 2011; Yu *et al.*, 2007; Luutserma, 1997 and Moya, 2012).

## 2.2 Preparation of bulk samples

For the preparation of the bulk ferroelectric samples of BNT and BNTL (BNT doped with lanthanum), percentages of 0.0, 0.3, 0.6, 0.8, 1.0, 3.0 and 6.0% of lanthanum (molar percent) are introduced into the structure of pure BNT. First, the precursor solution was dried at a temperature of 150°C/7hrs in a heating plate to obtain powders, then these powders were grounded manually in an agate mortar with which pellets were formed using a 1/2" die and a hydraulic press at 5885 Pa. The pellet samples are subjected to a heat treatment for calcination at 700 °C/1hr in order to obtain the desired perovskite phase. Then they are subjected to sintering in order to densify the bulk samples, the sintering was carried out in a tubular furnace with controlled temperature at 1060°C/1hr (Kim *et al.*, 2005, Kim *et al.*, 2003, Mayén *et al.*, 2013 and Leclerc, 1999).

## 2.3 Deposit of electrodes

Both BNT and BNTL bulk samples were prepared with metallic contacts (electrodes) to perform the respective ferroelectric measurements. Silver colloidal paint was placed on both sides of the cylindrical pellets manually, and then dried at 200 °C/20 min, with the purpose of adhering the contacts to the sample and being able to carry out the ferroelectric characterization.

## 2.4 Characterization techniques

The structural characterization by XRD was carried out in a Rigaku Dmax2100 X-ray diffractometer, operating with a step size of 5°, a voltage of 40 kV and a current of 30 mA. The Raman spectroscopy measurements were performed in an equipment with the following characteristics: High resolution spectrometer Spex-1403 with double holographic grids of 1800 lines/mm, and a resolution of 0.15 cm<sup>-1</sup>. An argon laser multiline Lexel was used with an excitation line source at 488 nm. The ferroelectric characterization was made with a Precision LC

equipment from Radiant Technologies Inc. coupled with a high voltage Trek source model 609E-6. Finally, the morphological characterization was made in a scanning electron microscope (SEM) model XL30 ESEM Philips, in backscattered electron mode (BSE) at a magnification of 1000x and 5000x, with a voltage of 12KV and 20 mA.

## 3 Results and discussion

Starting from BNT precursor solution (which we will call Formulation A, with sodium (Na<sup>+</sup>) and bismuth (Bi<sup>3+</sup>) in the same atomic ratio of 1:1). The samples were characterized by X-ray diffraction in order to verify the obtained perovskite phase of sintered BNT samples. Using the JADE software, it was possible to compare the diffraction patterns obtained from the measurement of the bulk samples with respect to those of the database. Figure 1 shows the XRD pattern of the formulation A of BNT, here we can observe a mixture of the perovskite phase of BNT, and a secondary phase known as "pyrochlore" corresponding to the composition Bi<sub>2</sub>Ti<sub>2</sub>O<sub>7</sub> (Gorfman *et al.*, 2010; Navarro *et al.*, 2010). These results were verified with the files: PDF # 32-0118 for the case of the pyrochlore phase (Bi<sub>2</sub>Ti<sub>2</sub>O<sub>7</sub>) and PDF # 36-0340 for the perovskite phase of BNT (Bi<sub>0.5</sub>Na<sub>0.5</sub>TiO<sub>3</sub>).

In order to quantify the chemical composition of the samples made with the formulation A, elementary chemical quantification measurements were made by dispersive energy spectroscopy of X-rays (EDS). According to the formula of the compound (Bi<sub>0.5</sub>Na<sub>0.5</sub>TiO<sub>3</sub>), sodium (Na<sup>+</sup>) and bismuth (Bi<sup>3+</sup>) must be in the same atomic ratio of 1:1.

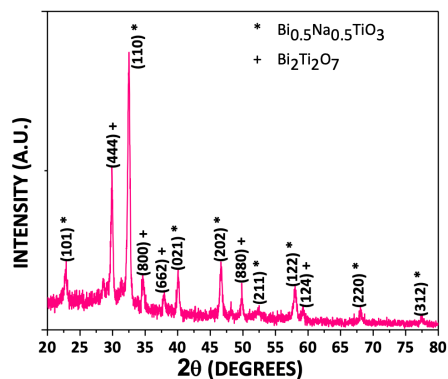


Fig. 1. XRD pattern of the formulation A of BNT

However the EDS results show that bismuth (At%) is present in almost the double of the atomic percentage with respect to the amount of sodium ( $\text{Na}^+$ ). This indicates that during heat treatment there is a loss of sodium, thus it was necessary to modify the initial concentration of sodium in the solution, and 100% excess of sodium ( $\text{Na}^+$ ) was added to stabilize the ratio between Na and bismuth ( $\text{Bi}^{3+}$ ).

A new BNT precursor formulation was made using the same precursor materials used in formulation A, however, in this case 100% excess of sodium ( $\text{Na}^+$ ) was added and we call this formulation B. The XRD pattern for a sample obtained from the formulation with an excess of sodium ( $\text{Na}^+$ ) (formulation B), shows that it was possible to obtain the pure perovskite phase of BNT without additional phases (figure 2). Furthermore, through an analysis performed with JADE software it was concluded that a BNT system with rhombohedral structure with an identification card PDF # 01-080-8493 was obtained, with lattice parameters ( $a$ ) = 5.480 Å and ( $c$ ) = 13.507 Å and a density of 5.492 g/cm<sup>3</sup>; determined by the Archimedes method, which correspond to a 91.83% of the theoretical density.

Once it was possible to establish the formulation for the elaboration of the BNT system without pyrochlore phase (formulation B), BNT doping with lanthanum ( $\text{La}^{3+}$ ) was carried out at 0.3, 0.6, 0.8, 1.0, 3.0 and 6.0% (atomic percentage); in order to evaluate the influence of the incorporation of La in its structural and ferroelectric properties (Krishnan *et al.*, 2011; Xiao *et al.*, 2013; Selvamani *et al.*, 2011).

Figures 2 and 3 show the XRD patterns for BNT samples doped with  $\text{La}^{3+}$  to the concentrations mentioned above. According to the diffractogram, it can be concluded that as the amount of lanthanum increases a second pyrochlore type phase ( $\text{Bi}_2\text{Ti}_2\text{O}_7$ ) appears. According to Mei Ling *et al.* (2014); this second phase occurs while the amount of lanthanum increases (specifically around 3.0 to 6.0%), however this pyrochlore phase usually disappears after sintering, except in the case of high percentages (above 3.0%) this does not happen. This means that there is a certain range around 0.6% substitution with lanthanum, which has a limit to enter into the structure of BNT, and the introduction of higher concentrations results in the formation of the pyrochlore phase.

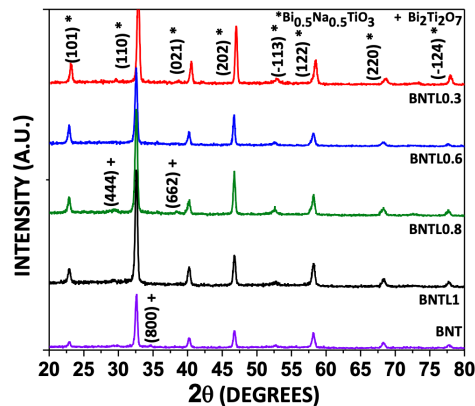


Fig. 2. XRD for BNT samples doped with lanthanum from 0 to 1.0% M. The samples are free of secondary phases until 0.6% M of La.

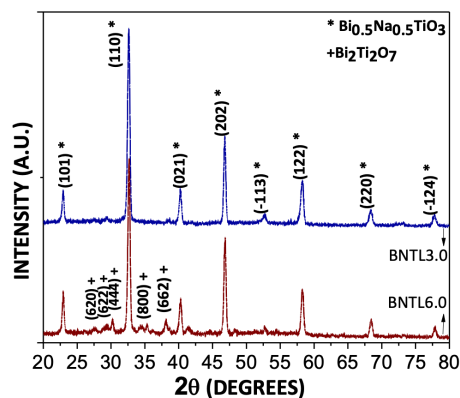


Fig. 3. XRD for BNT bulks doped with 3% and 6% M of lanthanum.

A refining analysis of XRD patterns with the software Materials Analysis Using Diffraction (MAUD) was carried out, which determined the evolution of the crystallite size as well as the variation of the lattice parameters for the rhombohedral structure, as a function of the concentration of lanthanum (Table 1).

From pure BNT, the crystallite size increases until it reaches 0.8% and 1.0% of lanthanum where it presents a considerable decrease with a similar value to pure BNT. However, for 3.0% and 6.0% of lanthanum, the size of the crystallite increases again appreciably, apparently the excess of lanthanum promotes the growth of the crystalline regions of the BNT, together with the appearance of the pyrochlore phase.

The analysis of the behavior of the grain size as a function of the concentration of lanthanum was carried out by scanning electron microscopy (SEM).

Table 1. Variation of the lattice parameters, crystallite size and grain size with respect to the concentration of lanthanum in BNT with rhombohedral structure.

Sample	Parameter a (Å)	Parameter c (Å)	Crystallite size (nm)
BNT PURE	5.489	13.507	66.904
BNT 0.3%	5.486	13.557	89.848
BNT 0.6%	5.486	13.557	89.846
BNT 0.8%	5.489	13.554	69.159
BNT 1%	5.485	13.522	62.476
BNT 3%	5.481	13.528	89.9
BNT 6%	5.479	13.490	82.925

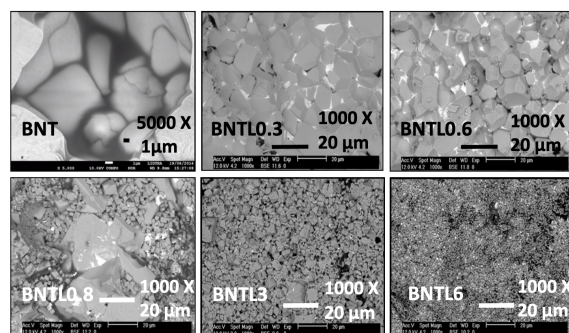


Fig. 4. SEM micrographs for BNT samples doped with 0.3-6% lanthanum.

The morphological evolution can be observed in figure 4, where for a concentration of 0.3% M an increase in grain size is observed, and for higher lanthanum concentrations, there is a decreasing tendency of the grain size, see Table 1. This may be because lanthanum  $\text{La}^{3+}$  substitutes the A sites in the structure of sodium  $\text{Na}^+$  and bismuth  $\text{Bi}^{3+}$ . Therefore due to its ionic radius it is close to Bi. It is probable that La substitutes Bi and reduces the Bi vacancies promoting the growth of the grain size, however, by increasing the amount of lanthanum ( $> 0.8\%$ ) Bi is segregated and forms the identified phase of  $\text{Bi}_2\text{Ti}_2\text{O}_7$ , reducing the grain size (Grimes *et al.*, 1999).

Raman spectroscopy of BNT doped with lanthanum was carried out in the concentrations mentioned above. The XRD patterns for all samples coincided with a rhombohedral structure, corroborating with this the introduction of the dopants within the BNT lattice.

It has been reported that the Rhombohedral structure for BNT ceramics has 13 active Raman modes and these are represented as  $\Gamma_{\text{RAMAN}} = 4A1 + 9E$ , which have been analyzed and reported by Petzelt *et al.* (2004).

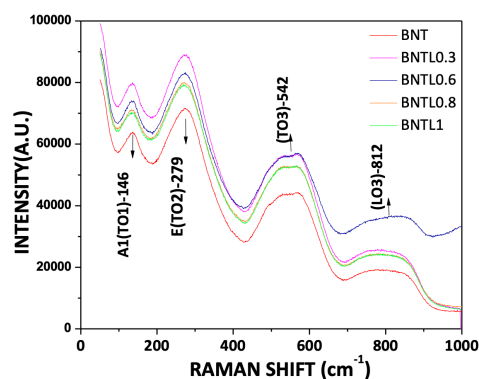


Fig. 5. Raman spectrum for BNT bulks doped with 0.0, 0.3, 0.6, 0.8 and 1.0% lanthanum

However, experimentally it is only possible to see four wide bands in a range from 100 to 1000  $\text{cm}^{-1}$  as shown in figure 5 for BNT doped with lanthanum from 0% to 1%. Figure 6 shows the Raman spectra obtained for the BNT sample with 3.0 and 6.0% of lanthanum. Here, it is possible to identify the representative bands of the BNT mentioned above in all cases. However, in the case of the BNT sample with 6.0% lanthanum an additional band (at around 450  $\text{cm}^{-1}$ ) was observed, which did not occur in any of the other samples. According to Navarro *et al.* (2010) the 447  $\text{cm}^{-1}$  band is attributed to the O-Ti-O bond, indicating the presence of  $\text{TiO}_2$  in the amorphous phase, which is an intermediate phase in the formation of  $\text{Bi}_4\text{Ti}_3\text{O}_{12}$ . However, according to the XRD pattern for this sample it was found that there is a pyrochlore phase  $\text{Bi}_2\text{Ti}_2\text{O}_7$ , which is a previous phase of  $\text{Bi}_4\text{Ti}_3\text{O}_{12}$ .

In order to clearly identify the Raman modes, the deconvolution of the spectrum was performed for a pure BNT system (Fig. 7), obtaining the following results (Petzelt *et al.*, 2004 and Parija *et al.*, 2013): Six bands are clearly identified in the spectrum near 135, 280, 530, 580, 770 and 830  $\text{cm}^{-1}$ .

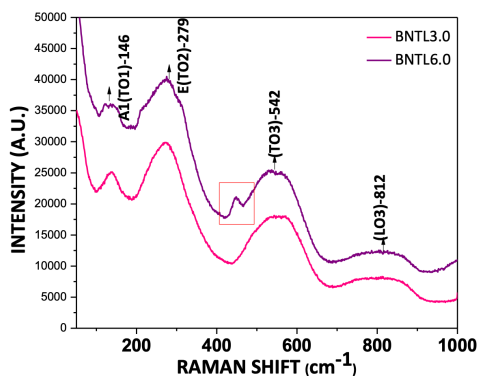


Fig. 6. Raman spectrum for BNT bulks doped with 3.0% and 6.0% of lanthanum.

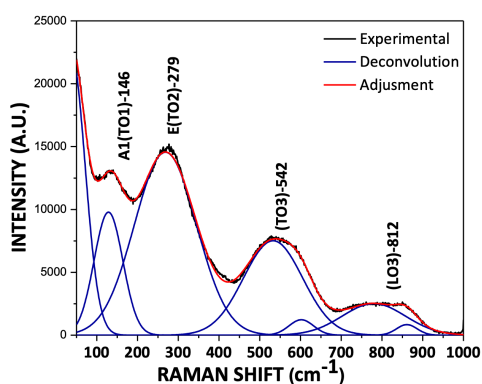


Fig. 7. Deconvolution of the Raman spectrum for a pure BNT system.

The bands around  $135$  and  $280\text{ cm}^{-1}$  are attributed to the vibrational modes of the Na-O and Ti-O bonds, due to the higher mass of the bismuth atom the band associated with the vibration of the Bi-O bond can fall at low frequencies and therefore is not present in these results. The bands present in  $135$  and  $280\text{ cm}^{-1}$  are sensitive to any structural transition and show a mode softening before any transition. Thus, it is evident that in all the systems obtained there is no structural transformation of BNT by the introduction of lanthanum. The bands near  $530$  and  $580\text{ cm}^{-1}$  are related to the vibration of the octahedron  $[\text{TiO}_6]$ . Finally, the bands at  $770$  and  $830\text{ cm}^{-1}$  are attributed to the distortions of the octahedrons  $[\text{TiO}_6]$  within the structure of the rhombohedral network. According to the XRD results, at these lanthanum concentrations an increase concentration of the pyrochlore phase of  $\text{Bi}_2\text{Ti}_2\text{O}_7$  is observed.

The ferroelectric parameters, polarization saturation ( $P_s$ ), remnant polarization ( $P_r$ ) and coercive field ( $E_c$ ), were obtained through hysteresis curves.

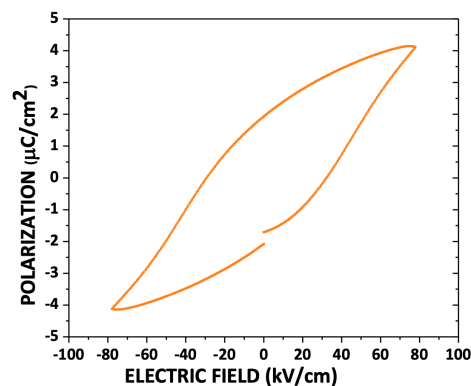


Fig. 8. Hysteresis curve for BNT pure sample obtained with formulation A, which show  $\text{Bi}_2\text{Ti}_2\text{O}_7$  as secondary phase.

In first instance, for the pure BNT system, low polarizations values were obtained, and these were not comparable with the polarizations of PZT. This could be due to the presence of structural defects in the material that can be attributed to a combination of porosity (from 90 to 95% with respect to the theoretical density) and deficiency of Bi. For this reason, it was proposed to carry out the high doping of lanthanum, in order to improve these results (Yeo H. *et al.*, 2009 and Jin L. *et al.*, 2014). It is worth noting that the results obtained for the samples that were initially made with the formulation (A) that gave rise to BNT with deficiency of sodium (Na) and with the pyrochlore phase ( $\text{BNT-Bi}_2\text{Ti}_2\text{O}_7$ ). The measurement of the hysteresis curve for the corresponding sample in volume, yielded the following results:  $P_s = 4.09\text{ }\mu\text{C}/\text{cm}^2$ ,  $P_r = 1.84\text{ }\mu\text{C}/\text{cm}^2$  and  $E_c = 34\text{ kV}/\text{cm}$ , compared with those obtained for BNT systems with lanthanum, which is by far one of the best ferroelectric results obtained (Fig. 8).

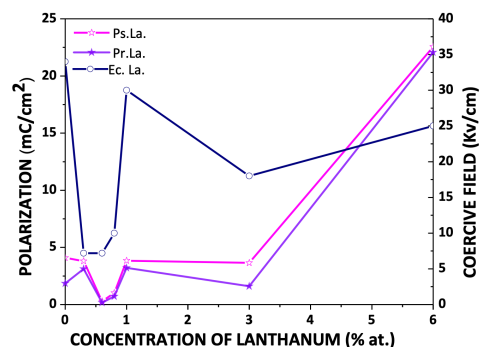


Fig. 9. Saturation Polarization Behavior ( $P_s$ ), Remnant Polarization ( $P_r$ ) and Coercive Field ( $E_c$ ) with respect to the increase of doping of lanthanum.

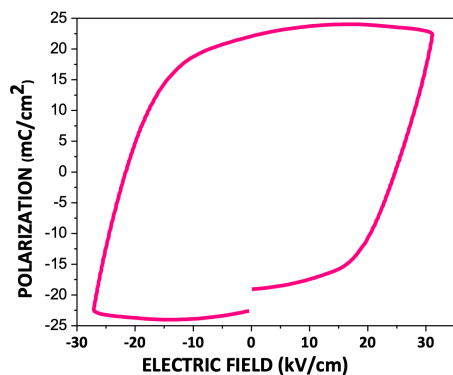


Fig. 10. Hysteresis curve for BNT sample doped with 6.0% lanthanum.

In the same way in figure 9, the ferroelectric behavior is summarized as a function of the increase of doping concentration of lanthanum. From this, it is concluded that doping up to 3%M did not improve the ferroelectric properties of the system, since lower values of  $P_r$  are obtained than those of the BNT without doping.

This may be due to the generation of vacancies during the process of incorporation of La in the sites of Bi, leading to porosity and segregation of the pyrochlore phase towards the grain boundaries. These defects lead to obtain Hysteresis curves with leaks, decreasing the polarization of saturation and remnant polarization.

However when substitution is made with 6.0% lanthanum, the highest values of  $P_r$  are presented for this set of samples and with an acceptable coercive field and lower than for pure BNT without doping. The ferroelectric parameter values are  $P_s=22.55 \mu\text{C}/\text{cm}^2$ ,  $P_r=22.06 \mu\text{C}/\text{cm}^2$  and  $E_c=25 \text{ kV}/\text{cm}$ . Additionally, according to the results of x-ray diffraction and Raman spectroscopy (figures 3 and 6), it could be concluded that the system with 6.0% lanthanum presented a BNT phase with pyrochlore ( $\text{Bi}_2\text{Ti}_2\text{O}_7$ ), with these results it can be said that the secondary phase of  $\text{Bi}_2\text{Ti}_2\text{O}_7$ , contributes to the ferroelectric properties of the material (remember Fig. 9) with a maximum polarization when doping with 6.0% lanthanum (fig. 10).

## Conclusions

This paper reports the synthesis of ferroelectric ceramics in volume of BNT with rhombohedral structure and density values around 90-92% of

theoretical density, made from powders obtained by the Sol-gel technique using the acetic acid route. The doping of BNT with lanthanum, showed that with high concentrations (0.8% - 6%) the samples present a secondary phase of pyrochlore  $\text{Bi}_2\text{Ti}_2\text{O}_7$ , which may be due to the fact that at high concentrations of the dopant, the lanthanum atoms can no longer be introduced into the crystal lattice of the BNT, causing as a result, a decrease in grain size and phase segregation with its increase; which was corroborated by XRD and Raman spectroscopy.

With respect to ferroelectric properties, the best responses were obtained for the pure BNT system with the presence of pyrochlore ( $\text{BNT-Bi}_2\text{Ti}_2\text{O}_7$ ) and BNT substituted with 6.0% lanthanum with the presence of pyrochlore as well. It is worth mentioning that in this case the concentrations at 0.3, 0.6, 0.8, 1.0 and 3.0% showed the lowest ferroelectric properties, which corroborates the positive contribution of the secondary phase in the ferroelectric properties of the material. Studies of the BNT system on its pyroelectric and relaxor properties are also the subject of studies in our group, due to their potential technological applications in energy storage systems.

## Acknowledgements

The authors are grateful to Dr. Rafael Ramírez Bon, the late Dr. Francisco Javier Espinoza Beltrán, Dr. Ma. Dolores Durruthy-Rodríguez and Dr. Francisco Calderón Piñar for their help in the discussion and results. Technical assistance is acknowledged by M.T. Rivelino Flores Farías, Q. in A. Martín Adelaido Hernández Landaverde, Eng. Francisco Rodríguez Melgarejo, Tec. Agustín Galindo Sifuentes, Eng. Carlos Alberto Ávila Herrera, Eng. José Eleazar Urbina Álvarez, and Adair Jimenez. The research was funded through the projects supported by CONACYT CB-2014-240460 and LIDTRA Lab-2014-01-254119 and LN-2018-295261. K. Moya Canul thanks CONACYT for the granted master's scholarship.

## References

- Cernea, M., Galca, A., Cioangher, M., Dragoi, C., Ionca, G. (2011). Piezoelectric BNT-BT0.11 thin films processed by sol-gel technique. *Journal of Mater and Science* 46, 5621-5627.

- Fernández, G. (2010). *Preparación y propiedades de láminas ultradelgadas policristalinas ferroeléctricas de PbTiO<sub>3</sub>*. Tesis de Doctorado en Universidad Autónoma de Madrid, Madrid España.
- Gorfman, S., Thomas P.A. (2010). Evidence for a non-rhombohedral average structure in the lead-free piezoelectric material Na<sub>0.5</sub>Bi<sub>0.5</sub>TiO<sub>3</sub>. *Journal of Applied Crystallography* 43, 1409-1414.
- Haertling, H.G. (1999). Ferroelectric ceramics: History and technology. *Journal of American Ceramic Society* 84, 797-818.
- Jaita, P., Watcharapasorn, A., Jiansirisomboon, S. (2011). Effects BNT compound incorporated on structure and electrical properties of PZT ceramic. *Current Applied Physics* 11, S77-S81.
- Jaffe B., Cook W.R. Jaffe H. (1971). Piezoelectric ceramics. *Journal of Sound and Vibration* 20, 562-563.
- Jaffe H., Berlincourt D. A., (1965). Piezoelectric transducer materials. *Proceedings of the IEEE* 53, 1372-1386.
- Jin I., Li F. y Zhang S. (2014). Decoding the fingerprint of ferroelectric loops: Comprehension of the material properties and structures. *Journal of American Ceramic Society* 97, 1-27.
- Khairunisak, A. R., Wai, C.S., Chai, Y. (2016). Properties of ce-doped Bi<sub>0.5</sub>Na<sub>0.5</sub>TiO<sub>3</sub> synthesized using the soft combustion method. *Procedia Chemistry* 19, 816-821.
- Kim, C.Y., Sekino, T. Yamamoto, Y., Niihara K. (2005). The synthesis of lead-free ferroelectric Na<sub>0.5</sub>Bi<sub>0.5</sub>TiO<sub>3</sub> thin film by solution-sol-gel method. *Journal of Sol-Gel Science and Technology* 33, 307-314.
- Kim, C. Y., Sekino, T., Niihara K. (2003). Synthesis of bismuth sodium titanate nanosized powders by solution/sol-gel process. *Journal of American Ceramic Society* 86,1464-1467.
- Krishnan, K., Sing, B.K., Gupta, M.K., Sinha, N., Kumar B. (2011). Enhancement in dielectric and ferroelectric properties of lead free Bi<sub>0.5</sub>(Na<sub>0.5</sub>K<sub>0.5</sub>)<sub>0.5</sub>TiO<sub>3</sub> ceramics by Sb-doping. *Ceramics International* 37, 2997-3004.
- Leclerc B. (1999). *Process optimization for sol-gel PZT films*. Master's thesis, Queen's University, Ontario Canada.
- Lucheng, Li., Mengxing, X., Qi, Z., Ping, C., Ningzhang, W., Dingkang, X., Biaolin, P, Laijun, L. (2018). Electrocaloric effect in L-doped BNT-6BT relaxor ferroelectric ceramics. *Ceramics International* 44, 343-350.
- Lutserma, G.A. (1997). *Spin coating for rectangular substrates*. Master's thesis, University of California, Berkeley, Estados Unidos.
- Martínez, J.R., Ruiz, F., De la Cruz, J. A., Villaseñor P. (1999). Formación y caracterización de materiales vítreos preparados por la técnica sol gel. *Revista Mexicana de Física* 45, 472-479.
- Mayén, R., Yañez, J. M., Moya, K. M., Herrera, A., Vazquez, M., Espinoza, F., López, A. M. (2013). Characterization of lead zirconate titanate (53/47) films fabricated by a simplified sol-gel acetic-acid route. *Journal of Materials Science* 24, 1981-1988.
- Mei, ling C., Khairunisak, A., Chai, Y. (2014). Properties of lanthanum-doped bismuth sodium titanate (Na<sub>0.5</sub>Bi<sub>0.5</sub>TiO<sub>3</sub>) prepared by soft combustion technique. *Advanced Materials Research* 858, 141-146.
- Meng, S., Wenru, L., Ming-Yu, L., Huan, L., Jianmei, X., Shiyong, Q., Guangzu, Z., Zixiao, L., Honglang, L., Shenglin J. (2019). High room-temperature pyroelectric property in lead-free BNT-BZT ferroelectric ceramics for thermal energy harvesting. *Journal of the European Ceramic Society* 39, 1810-1818.
- Moya, C. K. (2012). *Obtención y Caracterización de Películas delgadas Ferroeléctricas (PZT y BaTiO<sub>3</sub>) por la ruta Sol-gel empleando inmersión (dip coating) y rotación (spin coating)*. Tesis de Licenciatura, Universidad Autónoma de Sinaloa, Culiacán Sinaloa México.
- Navarro, M.G., Romero, J.J., Rubio, F. & Fernandez, J.F. (2010). Intermediate phases formation during the synthesis of Bi<sub>4</sub>Ti<sub>3</sub>O<sub>12</sub> by solid state reaction. *Ceramics International* 36, 1319-1325.



- Parija, B., Badapanda, T., Rout, S. K., Cavalcante, L.S., Panigrahi, S., Longo, E., Batista, N.C., Sinha T. P. (2013). Morphotropic phaseboundary and electrical properties of  $1-x[\text{Bi}_{0.5}\text{Na}_{0.5}]\text{TiO}_3 - x\text{Ba}[\text{Zr}_{0.25}\text{Ti}_{0.75}]\text{O}_3$  lead-free piezoelectric ceramics. *Ceramics International* 39, 4877-4886.
- Peng, F., Zhijun, X., Ruiqing, C. & Wei L. (2010). Piezoelectric, ferroelectric and dielectric properties of  $\text{La}_2\text{O}_3$ -doped  $(\text{Bi}_{0.5}\text{Na}_{0.5})_{0.94}\text{Ba}_{0.06}\text{TiO}_3$  lead-free ceramics. *Materials & Designs* 31, 796-801.
- Petzelt, J., Kamba, S., Fabry, J., Noujni, D., Porokhonsky, V., Pashkin, A., Kugel, G.E. (2004) Infrared, Raman and high-frequency dielectric spectroscopy and the phase transitions in  $\text{Na}_{0.5}\text{Bi}_{0.5}\text{TiO}_3$ . *Journal of Physics: Condensed Matter* 16, 2719-2731.
- Prado-Espinosa, A., Castro, M., Ramajo, L. (2017) Influence of secondary phases on ferroelectric properties of  $\text{Bi}_{0.5}\text{Na}_{0.5}\text{TiO}_3$  ceramics. *Ceramics International* 43, 5505-5508.
- Rodel, J., Jo, W., Seifert, K.T.P., Anton, E. M., Granzow, T., Damjanovic, D., (2009). Perspective on the development of lead-free piezoceramics. *Journal of American Ceramic Society* 92,1153-1177.
- Selvamani, R., Singh, G., Sathe, V., Tiwaril, V.S., Gupta, P.K. (2011). Dielectric, structural and raman studies on  $(\text{Na}_{0.5}\text{Bi}_{0.5}\text{TiO}_3)(1-x)(\text{BiCrO}_3)_x$  ceramic. *Journal of Physics: Condensed Matter* 23, 055901-8pp
- Smolenskii, G.A., Isupov, V. A., Agranovskaya, A. I., Krainik, N. N., (1961). New ferroelectrics of complex composition. *IV Soviet Physics Solid State*, 2651-2654.
- Tirado, G. S. (2015).  $\text{SnO}_2$ : Thin films prepared by sol-gel applied as propane gas sensors. *Revista Mexicana de Ingeniería Química* 14, 691-701
- Grimes, W., Grimes, R. W.(1999). Dielectric polarizability of ions and the corresponding effective number of electrons. *Journal of Physics: Condensed Matter* 10.;3029-3034
- Xiao, M., Lihong, X., Li, W., Shengming, Y., Qilai, Z., Youwei, Y. (2013). Synthesis, sintering, and characterization of BNT perovskite powders prepared by the solution combustion method. *Ceramics International* 39, 8147-8152.
- Xing-Yu, K., Zhi-Hao, Z., Yu-Kai, L.,Yeijing, D. (2019). BNT-based multi-layer actuator with enhanced temperature stability. *Journal of Alloys and Compounds* 771, 541-546
- Yeo, H., Sung, Y., Song, T., Cho, J., Kim, M. (2009). Donor doping effects on the ferroelectric and the piezoelectric properties of Pb-free  $\text{Na}_{0.5}\text{Bi}_{0.5}\text{TiO}_3$  ceramics. *Journal of Korean Physics Society* 54, 896-900.
- Yu, T., Kwok, K.W., Chan, H.L.W. (2007). Preparation and properties of sol-gel-derived  $\text{Na}_{0.5}\text{Bi}_{0.5}\text{TiO}_3$  lead-free ferroelectric thin film. *Thin Solid Film* 515, 3563 -3566.
- Yugong,W., Zhang, H., Zhang, Y., Jinyi, M., Daohua, X. (2009). Review enviromental friendly lead free-piezoelectric materials. *Journal of Material and Science* 44, 5049-5062.